INT. J. REMOTE SENSING, 2002, VOL. 23, NO. 13, 2537–2562

Taylor & Francis
Taylor & Francis Group

Vegetation and soil lines in visible spectral space: a concept and technique for remote estimation of vegetation fraction

A. A. GITELSON[1,2], R. STARK[2], U. GRITS[2], D. RUNDQUIST[1], Y. KAUFMAN[3] and D. DERRY[1]

[1]Center for Advanced Land Management Information Technologies, School of Natural Resource Sciences, University of Nebraska-Lincoln, Lincoln, NE 68588–0517, USA
[2]Department of Geological and Environmental Sciences, Ben-Gurion University of the Negev, Beer-Sheva, Israel
[3]NASA Goddard Space Flight Center, Greenbelt, Maryland, MD 20771, USA

(*Received 28 August 2000; in final form 7 June 2001*)

Abstract. The goal of this study is to investigate the information content of reflectance spectra of crops in the visible and near infrared range of the spectrum and develop a technique for remote estimation of vegetation fraction (*VF*). For four wheat species with $VF = 100\%$ in a wide range of pigment contents and compositions, a high degree of covariance was found for paired reflectances (R) at 550 nm versus 700 nm (R_{550} versus R_{700}) and 500 nm versus 670 nm (R_{500} versus R_{670}). Both relationships, defined as 'vegetation lines', were linear with determination coefficients $r^2 > 0.9$ and the plotted points were tightly clustered. Using the same coordinates to plot reflectances for a variety of soils, a high degree of covariance ($r^2 > 0.94$) and a distinct 'soil line' were found. The vegetation and soil lines define a two-dimensional spectral construct within which canopy reflectances, regardless of *VF*, may be located. Based on these optical properties of vegetation and soils, an attempt was made to estimate *VF* remotely for selected plant canopies. It is suggested that the coordinate location within the constructs, as defined by reflectances at 500 nm and 670 nm as well as at 550 nm and 700 nm, be used to measure *VF*. Algorithms for *VF* assessment in wheat for a wide range of soil brightness were devised and validated. The root mean square error (RMSE) of *VF* prediction was less than 10%. The technique was also validated by means of independent datasets taken above cornfields in Nebraska. The RMSE of *VF* prediction did not exceed 9.7%.

1. Introduction

One of the principal variables in the growth of crops is the fraction of the available solar radiation intercepted by foliage. The productivity of crops may be analysed as the product of the solar energy intercepted over a season and the efficiency with which that energy is converted to biomass. Steven *et al.* (1986) showed that in many crops the relationship between radiation interception and foliage cover is sufficiently close for the latter to be used as a substitute for more elaborate measurements of light interception.

There are three basic approaches for estimating vegetation fraction from satellite data: spectral mixture analysis (Adams and Smith 1986, Ustin *et al.* 1996), neural

International Journal of Remote Sensing
ISSN 0143-1161 print/ISSN 1366-5901 online © 2002 Taylor & Francis Ltd
http://www.tandf.co.uk/journals
DOI: 10.1080/01431160110107806

networks (Baret *et al.* 1995), and vegetation indices. Spectral mixture analysis with the use of reference end-members was employed to model reflectance data as mixtures of green vegetation, non-photosynthetic vegetation, soils, and shade (Roberts *et al.* 1993). It is an effective way to monitor vegetation cover. Linear spectral mixture modelling combined with principal component analysis has allowed the assessment of relevant agricultural and agronomic information in a natural scene using 10–20 spectral channels (Lelong *et al.* 1998). This technique requires ancillary ground measurements of pertinent biophysical variables in order to determine the empirical relationship between those variables and unmixing fractions for each different set of hyperspectral data. Other problems with spectral mixing were described by Price (1994).

Baret *et al.* (1995) successfully used neural networks to estimate canopy gap fraction and showed that it can be accurately estimated from NIR and red reflectances with the only ancillary information being the vegetation type and soil line characteristics. This 'black box' technique, which is dependent on the dataset used in the training process, performed better than the best vegetation index. They used a simulation model to provide a large dataset covering the possible range of variables. The main limitation of this approach results from the approximations and assumptions made in the modelling of the radiative transfer, and in the distribution of the input variables of the model. The vegetation fraction derived from the mixture modelling as well as from neural networks is not a straightforward estimation of the vegetation amount and requires careful analysis (Garcia-Haro *et al.* 1996).

Spectral vegetation indices are widely used indicators of temporal and spatial variations in vegetation structure and biophysical parameters (see reviews by Verstraete *et al.* 1996 and Moran *et al.* 1997 and references therein). This approach has already proven to be relevant to many requirements of vegetation status monitoring including assessment and monitoring of changes in canopy biophysical properties such as vegetation fraction (*VF*), leaf area index (LAI), fraction of absorbed photosynthetically active radiation, and net primary production (Asrar *et al.* 1984, Holben 1986, Myneni *et al.* 1995, 1997, Sellers 1985, Tucker 1979). Most vegetation indices combine information contained in two spectral bands, red and near-infrared (NIR). Considerable effort has been expended in improving the Normalized Difference Vegetation Index (NDVI) and in developing new indices to compensate both for the atmosphere (Kaufman 1989, Kaufman and Tanre 1992), and canopy background (Baret *et al.* 1989, 1993, Huete 1988, Huete *et al.* 1994). Nevertheless, the indices have limitations, some of which are due either to choices of band location and width (Sellers 1985, Yoder and Waring 1994, Gitelson *et al.* 1996, Myneni *et al.* 1997, Roberts *et al.* 1997), or to the fact that at midseason NI*R* reflectance levels off or even decreases with an increase of *VF* (see, for example, Colwell 1974, Daughtry *et al.* 1980, Kanemasu 1974, Jackson and Ezra 1985, Tucker *et al.* 1981). This behaviour prevents use of the NIR for estimation of moderate to high vegetation cover in crops.

A few authors have considered using only the visible range of the spectrum for estimating *VF*. Kanemasu (1974) found that NIR reflectance from wheat, sorghum, and soybean was highest at midseason and then levelled off and even decreased, while *VF* increased. He recommended using the ratio of reflectances at 545 and 655 nm as a measure of *VF* regardless of the crop type. Pickup *et al.* (1993) found, in the case of rangeland in Australia, that the red and NIR Landsat MSS bands allow much less separation of vegetation and soil than the green and red bands.

They developed a vegetation cover index using the green and red data space. That index was similar in form to the perpendicular vegetation index of Richardson and Weigand (1977), although Pickup *et al.* (1993) used only bands in the visible range of the spectrum. The index was calculated by identifying the soil line and determining the perpendicular distance of each pixel from that line. The distance was then scaled using distances calculated for points (or pixels) containing 100% vegetation cover. Kim *et al.* (1994) used high spectral resolution radiometry for remote sensing estimates of absorbed photosynthetically active radiation in vegetation canopies in the presence of nonphotosynthetic background material such as soil and leaf litter. They developed the chlorophyll absorption ratio index that utilized three spectral bands at 550 nm, 670 nm and 700 nm. To estimate *VF*, Gitelson *et al.* (2002) suggested using visible atmospherically resistant indices in the forms $VARI_{green} = (R_{green} - R_{red})/(R_{green} + R_{red} - R_{blue})$, and $VARI_{700} = (R_{700} - 1.7*R_{red} + 0.7*R_{blue})/(R_{700} + 2.3*R_{red} - 1.3*R_{blue})$, where R_{blue}, R_{green}, and R_{red} are reflectances in MODIS spectral channels, and R_{700} is reflectance in the MERIS (695–705) spectral channel. The index was found to be linearly dependent on wheat and corn *VF*.

Strong relationships between reflectance at 550 nm (R_{550}) and at 700 nm (R_{700}) were found for leaves of different and unrelated plant species (Chappelle *et al.* 1992, Gitelson and Merzlyak 1994a, b, 1996, McMurtrey III *et al.* 1994). The reflectance ratio R_{550}/R_{700} was found to be virtually constant regardless of the differences in chlorophyll and carotenoids content. Similarity between R_{550} and R_{700} could be understood if pigments occurring exactly in the same proportion affect the absorption at these wavelengths (Gitelson and Merzlyak 1996). In the range 550 nm to 700 nm, both Chl-a and Chl-b play a major, even dominant, role in light absorption. Among the carotenoids present in the chloroplasts of higher plant leaves, only β-carotene exhibited absorbance at 550 nm, but in an extremely small amount (Lichtenthaler, 1987). In the presence of trace amounts of chlorophylls ($< 3\,mg\,m^{-2}$) and considerable quantities of carotenoids ($> 30\,mg\,m^{-2}$), there is no evidence for the contribution of the carotenoids to reflectance at 550 nm (Gitelson and Merzlyak 1996, Merzlyak *et al.* 1999). Reflectance at 700 nm is mainly a result of absorption by Chl-a; however, it cannot be ruled out that Chl-b also contributes to the absorption at 700 nm. Thus, the near-perfect covariance ($r^2 > 0.98$) between R_{550} and R_{700} is a result of a very close relationship between Chl-a and Chl-b and negligible absorption by carotenoids at 550 nm.

A strong degree of covariance between reflectances R_{670} and R_{500} for leaves in a wide range of pigment content and composition was reported (Gitelson *et al.* 1996). The ratio R_{670}/R_{500} remained constant for leaves with chlorophyll contents ranging from 150 to more than $700\,mg\,m^{-2}$. The exception to this occurs with strongly stressed or senescing (yellowing) leaves with low (below $150\,mg\,m^{-2}$) Chl content (Merzlyak *et al.* 1999). R_{500} is controlled by total pigment content (i.e. the combined absorption of Chl-a, Chl-b, and carotenoids), while R_{670} is governed solely by total Chl content (absorption by Chl-a and Chl-b). In slightly green to dark-green leaves, total Chl content and total pigment content vary almost synchronously; thus, the ratio of total pigment content to total Chl content remains practically constant in a wide range of pigment content and composition (Merzlyak *et al.* 1999). It explains the high correlation that exists between R_{500} and R_{670}.

Thus, it is reasoned that these relationships, inherent for leaf reflectance in (500, 670) and (550, 700) data spaces, might be applied to improve existing procedures for both identifying the vegetation end-member (versus soil) and assessing *VF*.

This article describes a technique for estimating *VF* based on reflectances in either the green (near 550 nm) and the red edge (near 700 nm) or the blue (around 500 nm) and the red (660–680 nm), both of which seem more robust in estimating crop vegetation cover than the red-infrared indices commonly used. Close-range radiometer data were collected and analysed in order to demonstrate how reflectance responded to targets representing a wide range of wheat *VF*. Then, the developed technique was validated by independent datasets for four wheat species. Finally, we document, based on radiometer data taken over cornfields in Nebraska, how the technique performed over an entire growing season. In this way, evidence can be provided of the extent to which the proposed techniques are affected by changes in vegetation greenness and canopy structure.

Thus, it is proposed to use only the visible range of the spectrum to estimate quantitatively *VF*, and link these findings to new satellite technologies and the high spectral and radiometric resolutions achieved in the recently launched SeaWiFS, MODIS, ASTER, MISR, and MERIS.

The approach taken was first to study the reflectance of wheat with 100% *VF* in order to test whether the leaf-level relationships (R_{670} versus R_{500} and R_{550} versus R_{700}) are valid at the canopy level. Subsequently, the variability in spectral responses from soils and wheat (with 100% *VF*) was investigated in two spectral spaces (500, 670) and (550, 700) as a means of assessing their utility as baselines against which vegetation growth and development could be quantitatively compared and analysed.

2. Methods and techniques

The study took place in agricultural fields near the city of Beer-Sheva, Israel (31°13′N; 34°48′E), located on the northern edge of the Negev Desert. The crops were irrigated on a regular basis by the water effluent from a nearby reservoir using sprinklers installed in straight parallel lines. In the first year, experiments were conducted from the middle of December 1997 until the middle of May 1998, and the crops consisted of four species of wheat (*T. aestivum*)Ð *'Ariel'*, *'Ayalon'*, *'Beit-Hashita'*, and *'Yaniv'*. The differences among the species is mainly in their purpose for growing—grains versus silage. There is also a difference in their physical parameters such as height and density of canopy. In the second year, experiments were conducted from the middle of November 1998 until the end of March 1999; one species of wheat was investigated—*'Ayalon'*. The data were collected over the course of the growing cycle (from seeding until harvesting), at one to two week intervals.

Radiometric data were collected close to solar noon (between 11am and 1pm); changes in solar zenith were minimal. Each measurement campaign (11 total in the 1997/98 season and 13 total in the 1998/99 season) took about an hour. Reflectance spectra were acquired within each field at a few randomly selected locations on each measurement date; measurement locations were not retained from one data-collection campaign to the next. Reflectance spectra were measured above the canopy using a high spectral resolution spectroradiometer, a Licor LI-1800, in the range 400 nm–1100 nm with a spectral resolution of 2 nm. To measure upwelling radiance of the canopy (L_{canopy}), the LI-1800 was attached to a telescope with a field of view (FOV) of 15°, which was positioned above the canopy at a height of about 2 m. The 15° optic resulted in an instantaneous field of view of about 50 cm by 50 cm at the top of the canopy. Measurements of upwelling radiance were repeated at least five times at each sampling station and the average value was used in the analysis. Each reading took approximately 25s. Upwelling radiance from a $BaSO_4$ panel (L_{ref}) was

measured and used as reference. A microcomputer initiated spectroradiometer scanning and stored the data. Then, in the laboratory, data were downloaded to the computer and the upwelling radiance from each vegetation-target scan was normalized to the appropriate upwelling radiance spectrum acquired over the reference panel.

Over the course of the growing season, solar elevation for the study site varied significantly (from 31.8°to 53°). Since the directional response of the reference panel is non-Lambertian (Jackson *et al.* 1992), the correction of anisotropic reflectance from the calibration target was made in accord with Sandmeier *et al.* (1998).

Reflectance spectra of soil were taken before and just after the planting in the same fields where the crops were grown. Measurements were made in at least 20 randomly selected locations per field and in a very wide range of soil moisture. Additional measurements of bare soil reflectance were taken between the wheat rows, when *VF* was less than 30%. The range of measured soil reflectance was very wide, and we are convinced that our measurements are representative of the soil during the growing season.

Colour photos (35 mm) were acquired over each plot at the same height as the radiometric scan with the same field of view, and the *VF* was estimated from these photos using an unsupervised classification module within the ERDAS Imagine image processing software. Canopy height and LAI (direct destructive measurements) were measured at the same spots where radiometric measurements were obtained.

The developed technique was validated by two independent datasets. The combined wheat database (reflectance spectra and *VF*, collected from December 1997 until the middle of May 1999) was separated into model development and model testing datasets. For the model development dataset, data collected in the 1997–1998 growing season for four wheat species *Ariel*, *Ayalon*, *Beit-Hashita*, and *Yaniv*, were used. Model validation was attempted using data collected in the 1998–1999 growing season for *Ayalon* wheat. Predicted *VF* was calculated using reflectance from the validation data set (blue: 459 nm–479 nm, green: 546 nm–556 nm, and red 620 nm–670 nm MODIS channels, and also the MERIS red edge channel: 700 nm–710 nm) with coefficients of equations generated for the model development data set. Root Mean Square Errors (RMSE) of *VF* prediction were estimated by comparing the predicted *VF*s with those retrieved by processing the digital-camera images.

Validation of the suggested technique was also carried out using data on corn reflectance and *VF*. The study area was the University of Nebraska Agricultural Research and Development Center (ARDC), located near Mead, Nebraska. The specific study site was a one-acre field of corn planted in a randomized design consisting of 16 plots (Derry 2000). Each plot measured 11.4 m × 12.2 m (37.5 ft × 40 ft) or approximately 135 m^2 (1500 ft^2).

Hyperspectral data for corn were collected at close range using a Spectron Engineering SE-590 portable spectroradiometer. The system detects and records spectral data in 252 usable bands with a spectral range from 365 nm to 1126 nm. Average wavelength spacing between midpoints of adjacent bands is about 3 nm. The sensor was configured to acquire eight individual radiance measurements, which were internally averaged and stored as a single data file. The controller is connected to a portable computer, which initiates the scanning procedure, graphically displays the reflectance values of the target, and stores the data. The sensor was positioned at a height of 5.8 m above the canopy and pointed due south to reduce shadowing. Data were collected close to solar noon (between 11 am and 3 pm) when changes in

solar zenith are minimal. The 15° optic resulted in an instantaneous field-of-view (IFOV) of 150 cm (diameter) at the top of the canopy. The sensor head was then positioned over six different, randomly selected sample locations within each plot and radiant flux was measured. Measurement locations were not retained from one data-collection campaign to the next. A white Spectralon (Labshere, Inc., North Sutton, NH) reflectance standard was used to calibrate the spectroradiometer to the total incoming radiant flux. All canopy radiance data were imported into Microsoft's Excel Spreadsheet software and the reflectance was calculated as: $R_{\lambda\,\mathrm{corn}}(\%) = (L_{\lambda\,\mathrm{corn}}\{\mu\mathrm{W\,cm^{-2}\,sr^{-1}\,nm^{-1}}\})/(L_{\lambda\,\mathrm{panel}}\{\mu\mathrm{W\,cm^{-2}\,sr^{-1}\,cm^{-1}}\})*100$, where $L_{\lambda\,\mathrm{corn}}$ is measured radiance for corn per wavelength, λ, $L_{\lambda\,\mathrm{panel}}$ is measured radiance for the calibration panel per wavelength, λ, $R_{\lambda\,\mathrm{corn}}$ is canopy reflectance (%) for corn per wavelength, λ.

Spectral data were collected at regular intervals (every three weeks) throughout the season, but atmospheric conditions dictated whether or not data were actually collected on the scheduled dates. As a result of weather, corn spectra were eventually collected at four stages of development. The reflectance values from the six sample locations within each plot were averaged, resulting in a single reflectance value, per wavelength, for each plot.

Digital camera images were acquired using a Kodak DC-40 system. The camera, mounted adjacent to the SE-590, provided above-canopy images from the view of the spectroradiometer. A digital image was acquired over each of the 16 plots concurrent with spectral data collection of the corn canopy. The digital camera images were imported into E*R*DAS Imagine (version 8.3.1) for processing. The area (size) and location of the SE-590 IFOV in each image was determined and a model was designed to exclude data outside the 152.5 cm diameter of the IFOV. The model also separated non-vegetation (soil) pixels from vegetation pixels by subtracting the green band from the red band. The images were recoded to create a file containing two classes: non-vegetation and vegetation.

3. Results

3.1. *Relationships* R_{500} *versus* R_{670} *and* R_{550} *versus* R_{700}

Averaged reflectance spectra of wheat taken in 8 to 16 sample locations during the course of a growing period are shown in figure 1. Reflectance in the visible spectrum decreased in an orderly fashion from emergence to heading stages. This decrease was most pronounced in the green and red ranges (550 nm–680 nm) and least pronounced in the blue (400 nm–500 nm). In the early stages of the growing season, a sharp decrease of reflectance occurred near 700 nm in the so-called 'red edge' region. NIR reflectance was highest at midseason and then leveled off and even decreased from almost 50% to nearly 35%, whereas canopy density and *VF* increased (Gitelson *et al.* 2002, Stark and Gitelson 1999, 2000).

As noted earlier, a very close relationship between paired reflectances at 500 nm and 670 nm and also at 550 nm and 700 nm was observed at leaf level. We were interested in determining whether or not the same relationships existed at the canopy level; so the first step was to study reflectance spectra acquired over the wheat fields with a *VF* of 100%. When *VF* reached 100%, LAI was measured at 7–8, but it continued to increase up to a surprisingly high 12 (the wheat was irrigated). When LAI was at about 7, both R_{550} and R_{700} were around 7% (figure 2(*a*)). Then, when LAI increased, both reflectances decreased synchronously reaching very small values at around 2% for LAI = 12. An increase in LAI led to an increase in light interception,

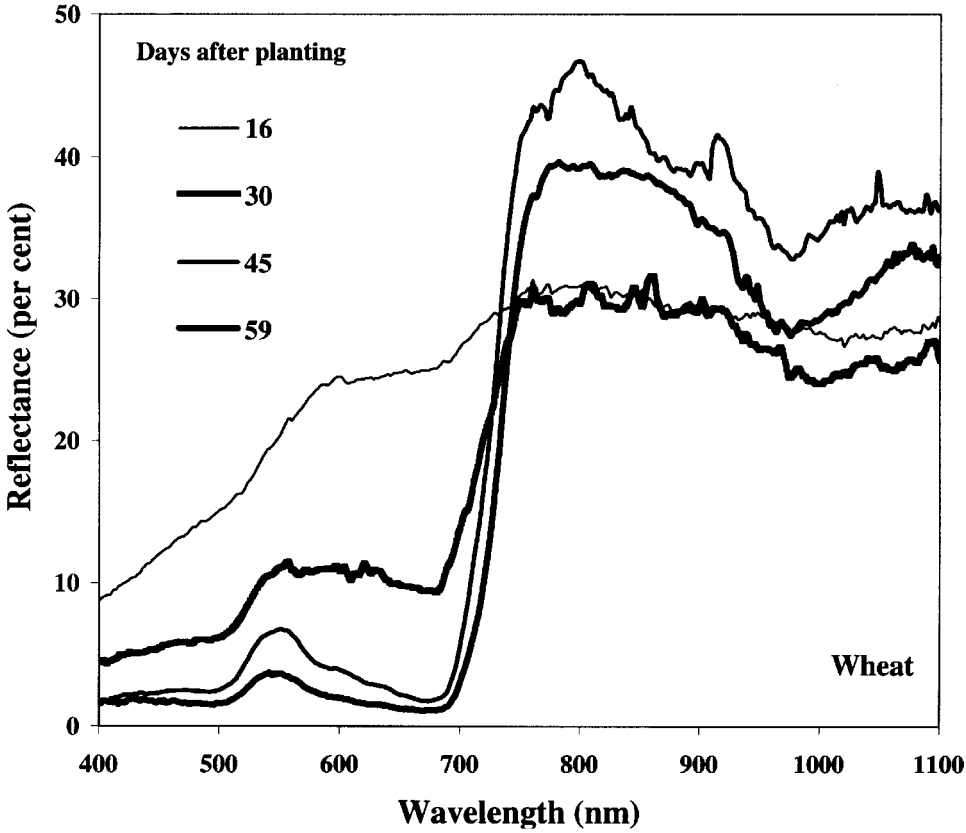

Figure 1. Reflectance spectra of wheat.

and thus an increase in absorption by the canopy. As a result, pigment content (per area of canopy) increased in proportion to that in leaves; absorption at 550 nm was determined by both Chl-a and Chl-b and at 700 nm solely by Chl-a (Chappelle *et al.* 1994, Gitelson and Merzlyak 1996). The functional similarity of the responses of light-harvesting pigments at these wavelengths causes the synchronous increase in absorption at 550 nm and 700 nm and synchronous decrease of R_{550} and R_{700} (figure 2(*a*)).

When *VF* reached 100% (and LAI was at 7–8), the reflectances R_{500} and R_{670} fell to very low level, approximately 2.5 to 3% (figure 2(*b*)). As LAI increased to 12, R_{500} and R_{670} decreased slightly reaching extremely small values (0.5%). As noted above, an increase in canopy density caused an increase in pigment content per area of canopy, and as was the case at leaf level, absorption in the blue range was determined by total pigment content (Chl-a, Chl-b, and carotenoids) and in the red by total Chl content (Chl-a and Chl-b). The strong correlation between total pigment content and total Chl content in light green to dark-green leaves explains the very close correlation between R_{500} and R_{670} (figure 2(*b*)).

When the canopy was closed, relationships R_{670} versus R_{500} as well as R_{550} versus R_{700} approximate a line in two-dimensional spectral space. For a wide range of canopy densities (LAI changed for a closed canopy from 7–8 to 12), structures and pigment contents, both relationships R_{700} versus R_{550} and R_{670} versus R_{500} were linear with determination coefficients $r^2 > 0.90$, and the plotted points were tightly

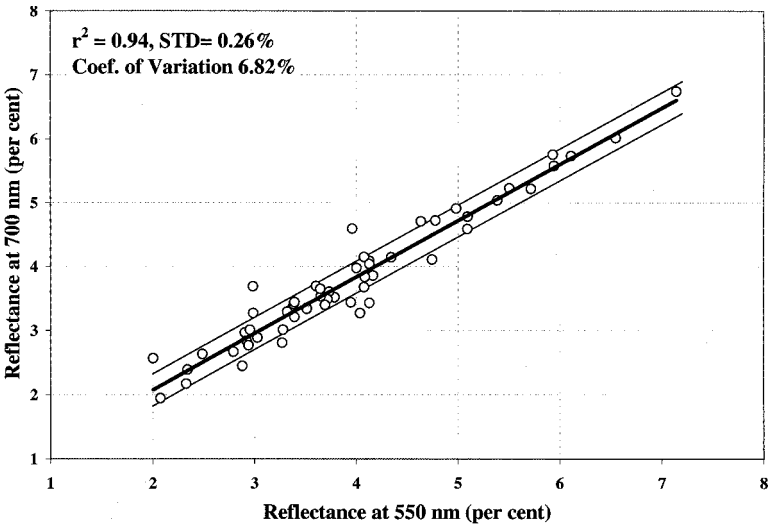

(*a*)

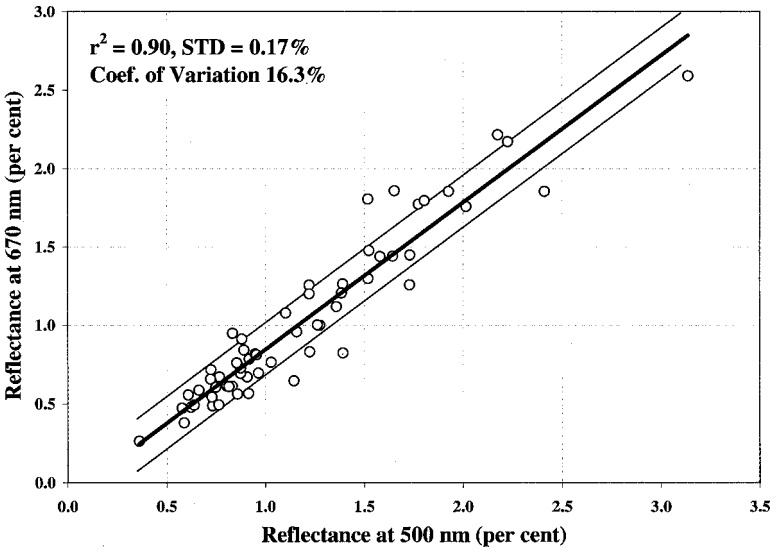

(*b*)

Figure 2. Reflectance of wheat with vegetation fraction 100% in spectral spaces: (*a*) R_{700} versus R_{550} ($R_{700} = 0.88R_{550} + 0.31$, $r^2 = 0.94$) and (*b*): R_{670} versus R_{500} ($R_{670} = 0.94R_{500} - 0.09$, $r^2 = 0.9$). Solid lines are best-fit functions. Thin lines show root-mean square errors of sample points from the linear relationship R_i versus R_j.

clustered. The standard deviation was less than 0.17% for the relationship R_{670} versus R_{500} and 0.26% for R_{550} versus R_{700}. Thus, for a canopy with $VF = 100\%$, the plotted scatter of 'vegetation points' constitute, in reality, a 'vegetation arc' or 'line'. Therefore, this relationship is referred to as the 'vegetation line.'

Soil brightness varied considerably. In the blue range, the reflectance varied between 3 and 22% and in the red edge range near 700 nm it varied between 8 and

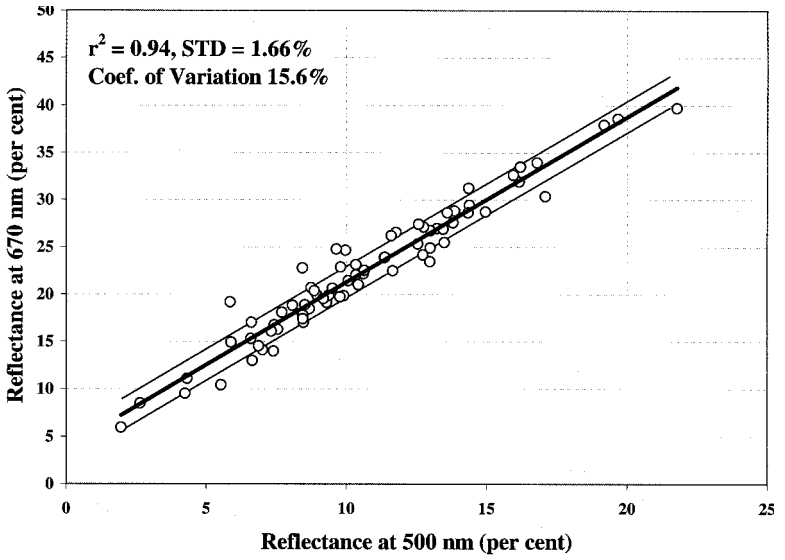

(*a*)

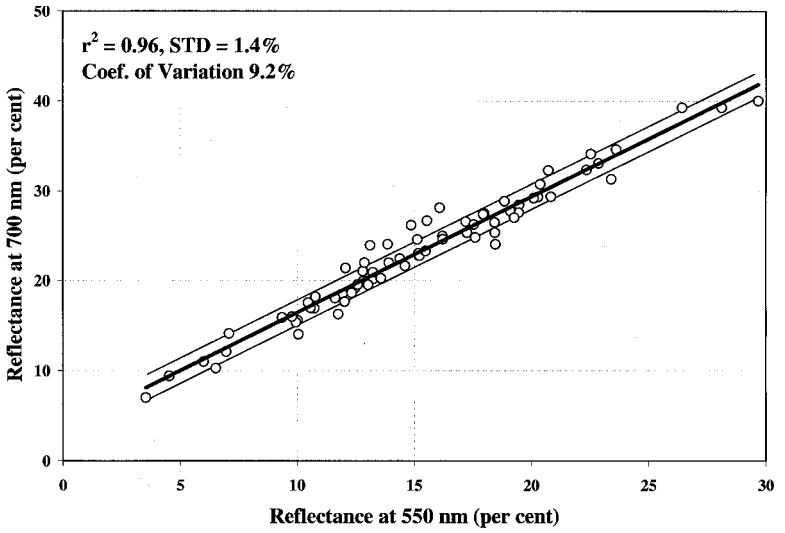

(*b*)

Figure 3. Reflectance of soils in spectral spaces: (*a*) R_{670} versus R_{500} ($R_{670} = 1.75R_{500} + 3.8$, $r^2 = 0.94$) and (*b*) R_{700} versus R_{550} ($R_{700} = 1.29R_{550} + 3.53$, $r^2 = 0.96$). Solid lines are best-fit functions. Thin lines show root-mean square errors of sample points from the linear relationship R_i versus R_j.

40%. Reflectance increased with wavelength and was, at least to some extent, a function of soil moisture. In a wide range of soil brightness, reflectances R_{670} and R_{500} correlated very closely ($r^2 = 0.94$, STD = 1.66%), forming a 'soil line' (figure 3(*a*)). A very strong degree of covariance ($r^2 = 0.96$; STD = 1.4%) was also found between reflectances R_{700} and R_{550} (figure 3(*b*)).

3.2. *Concept of vegetation fraction estimation*

Figure 4 shows the relationships R_{670} versus R_{500} and R_{700} versus R_{550} for wheat when *VF* ranged between 0 and 100%. Soil lines are the best-fit functions presented in figures 3(*a*) and 3(*b*). The vegetation lines in both spaces are formed by reflectance data acquired over wheat with $VF = 100\%$ (figures 2(*a*) and (*b*)). The variation of reflectance with *VF* was very pronounced. In (500, 670) spectral space, reflectance ranged from 2 to 15% at 500 nm and from 2 to nearly 30% at 670 nm (figure 4(*a*)). In (550, 700) spectral space, reflectance ranged even more: from 2 to 22% at 550 nm, and from 2 to nearly 30% at 700 nm (figure 4(*b*)).

The vegetation and soil lines define a two-dimensional spectral construct for each of the paired reflectances. For example, figure 5 depicts the case for reflectances at R_{550} and R_{700} for soil and wheat. Using the end points of both the vegetation and soil lines, we define area EFGH, within which canopy reflectance, regardless of *VF*, should be located. Our concept is to use the position of actually measured reflectance between the soil line and vegetation line, as a measure of *VF*. When the *VF* is near zero, the plotted point must be near or on the soil line. When the *VF* reaches 100%, the plotted point must be near or on the vegetation line. Points that are near or on the soil line and that have low reflectance, correspond to dark soils. Points that are near or on the soil line and that have high reflectance correspond to light-coloured soils. The same is essentially true for vegetation; those canopies that are 'bright' will be located at the end of the vegetation line having high reflectivity. The topology of this two-dimensional construct will change as vegetation brightness and soil colour change. The position of a point within this construct with the same *VF* will also change as the vegetation brightness and soil colour change. With our data, an increase in *VF* caused an orderly decrease in reflectance in both spectral spaces. An increase in *VF* beyond about 70% led to only a slight decrease in reflectance. Such behaviour is attributed, at least to some extent, to a 'shadowing effect' within the canopy of very dense wheat studied. Even though the soil in the Israeli study site was quite bright, soil contribution to reflectance decreased significantly by shadowing and the canopy reflectance was low. Thus, in spectral bands where the soil influence should have been an important part of the composite upwelling spectral signal (i.e. the red and the red edge near 700 nm), overall reflectance was low and quite similar to that of closed canopy.

To understand the dynamics of the two-dimensional construct, consider the following hypothetical situations. Assume that a sample of wheat reflectance at 550 nm and 700 nm was placed at point O in spectral space (R_i, R_j) (figure 5). The location at O could either be the result of a bright soil (e.g. point B) and dark green canopy (e.g. point C), or a much darker soil (e.g. point A) and a bright canopy (e.g. point D). Note that point O could be located the same in either case. Therefore, the *VF* may be expressed as the ratio of either AO/AD or BO/BC. Notice, too, that the vegetation and soil lines tend to be non-parallel in both spectral spaces; the slope of the vegetation line is slightly less than that of the soil line (figure 4). So, *VF* estimates depend upon both soil brightness and vegetation greenness. The segment of the soil line between points A and B represents the probable range of soil brightness for sample O. The segment of the vegetation line between points C and D represents the probable range of vegetation greenness. Thus, errors in estimating *VF* are likely to be caused by the range of variation of either soil (AB) or wheat (CD) reflectance (or both). *VF* may lie in the range of ratios AO/AD and BO/BC (figure 5). This difference depends also on the relative positions of the soil and vegetation lines. For

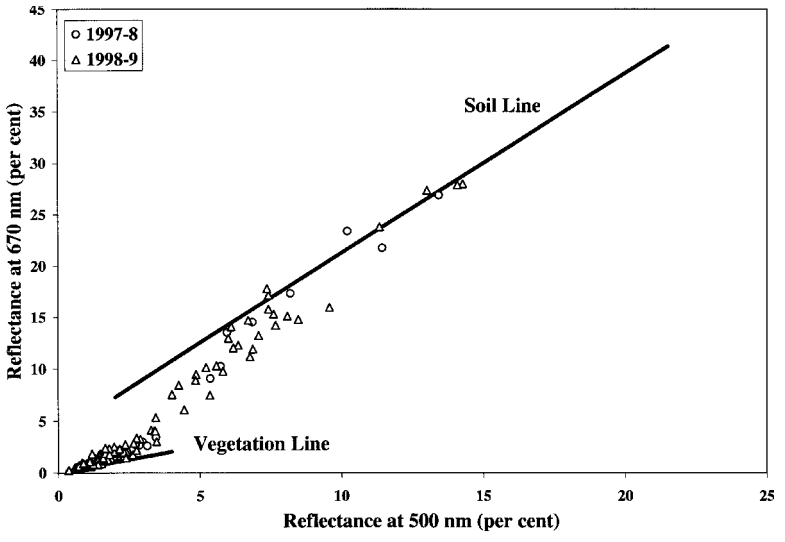

(*a*)

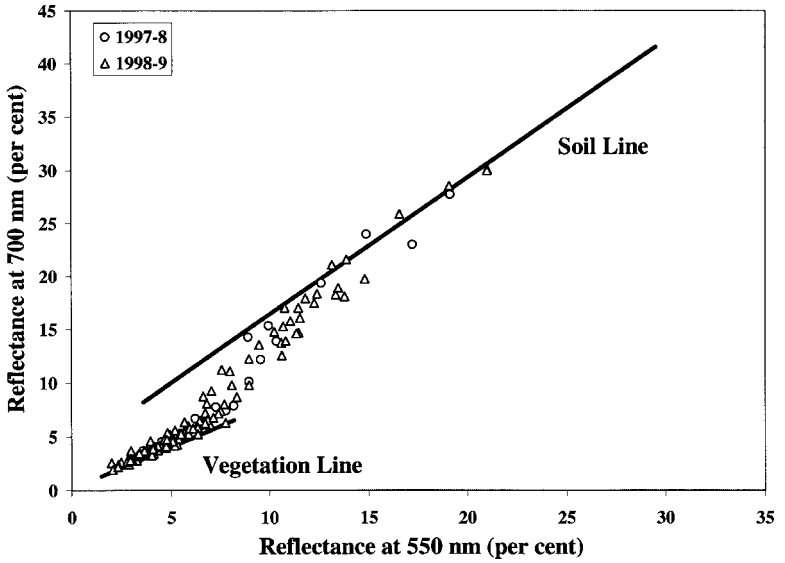

(*b*)

Figure 4. Reflectance of wheat with vegetation fraction from 0 to 100% in spectral spaces: (*a*) R_{670} versus R_{500} and (*b*) R_{700} versus R_{550}. Soil lines are best-fit functions presented in figures 3(*a*) and 3(*b*), vegetation lines are best-fit functions presented in figures 2(*a*) and 2(*b*).

the wheat studied, and the expected soil reflectance, the uncertainty of *VF* estimation might reach 6% in coordinates R_{700} and R_{550} and 10% in coordinates R_{670} and R_{500} (Gitelson *et al.* 2000).

In figure 6(*a*), point O represents reflectance of a wheat canopy with low *VF*. The plotted point is located just near the soil line. Actually measured reflectance may represent any vegetation within the constraint of the plotted soil and vegetation

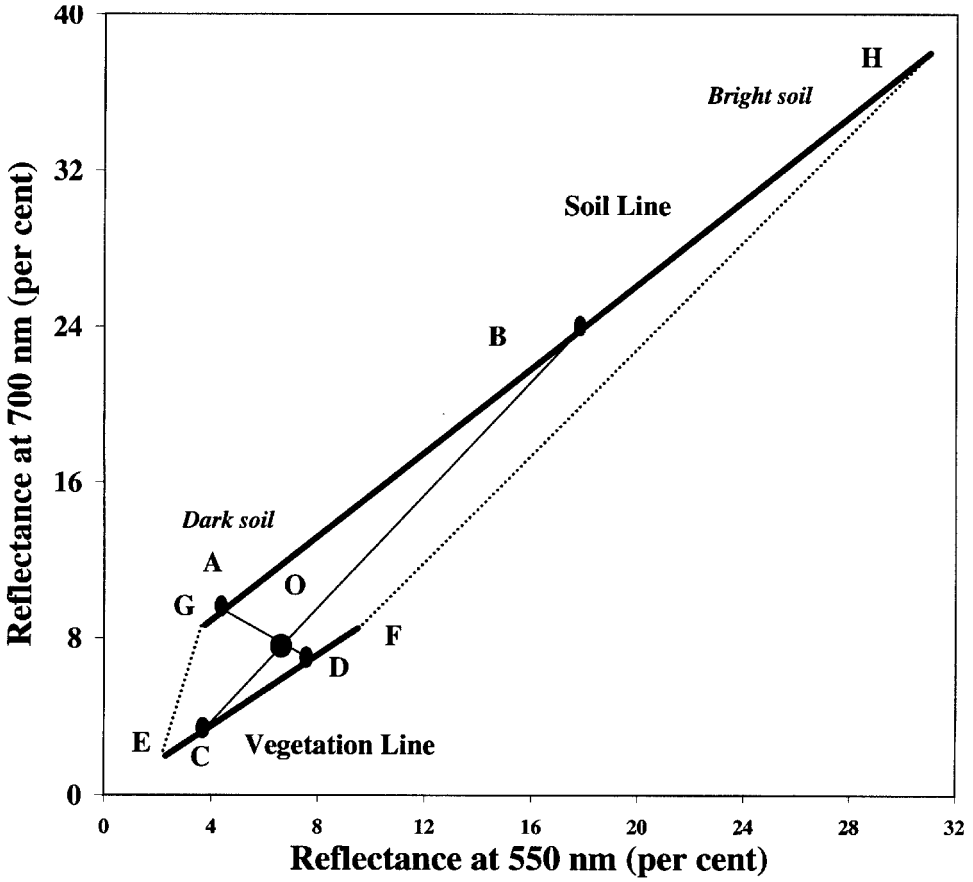

Figure 5. The range of possible vegetation greenness (c,d) and soil brightness (a,b) variation for pixel placed at point O in spectral space R_{700} versus R_{550}.

lines: vegetation greenness may vary in a wide range between points C and D. At the same time, the position of that point in spectral space leaves the possibility of only narrow variation in soil brightness that may range between points A and B. *VF* estimates may lie within a range limited by ratios AO/AD and BO/BC. The first ratio corresponds to the minimum possible for this example soil brightness (point A) and maximum possible for vegetation brightness (point D). The second ratio corresponds to maximum possible soil brightness and minimum vegetation brightness. For this case, *VF* may only be in the range 11.8% to 13.6%.

Point O in figure 6(*b*) shows reflectance of wheat with moderate *VF*. The range of probable vegetation greenness remained the same as in case (*a*), but the range of probable soil brightness may be much wider (AB is much longer than in the case (*a*)), and it increases the uncertainty of *VF* estimation. *VF* estimates lay within the range 45.4 to 52.4 defined by the ratios AO/AD and BO/BC.

Figure 6(*c*) illustrates the case of wheat with high *VF*. The point O is positioned just near the vegetation line. The range where probable soil brightness may lie is maximal, while the range of vegetation greenness is narrow. *VF* estimates for this case might lie in the range 87.5% to 91.9%.

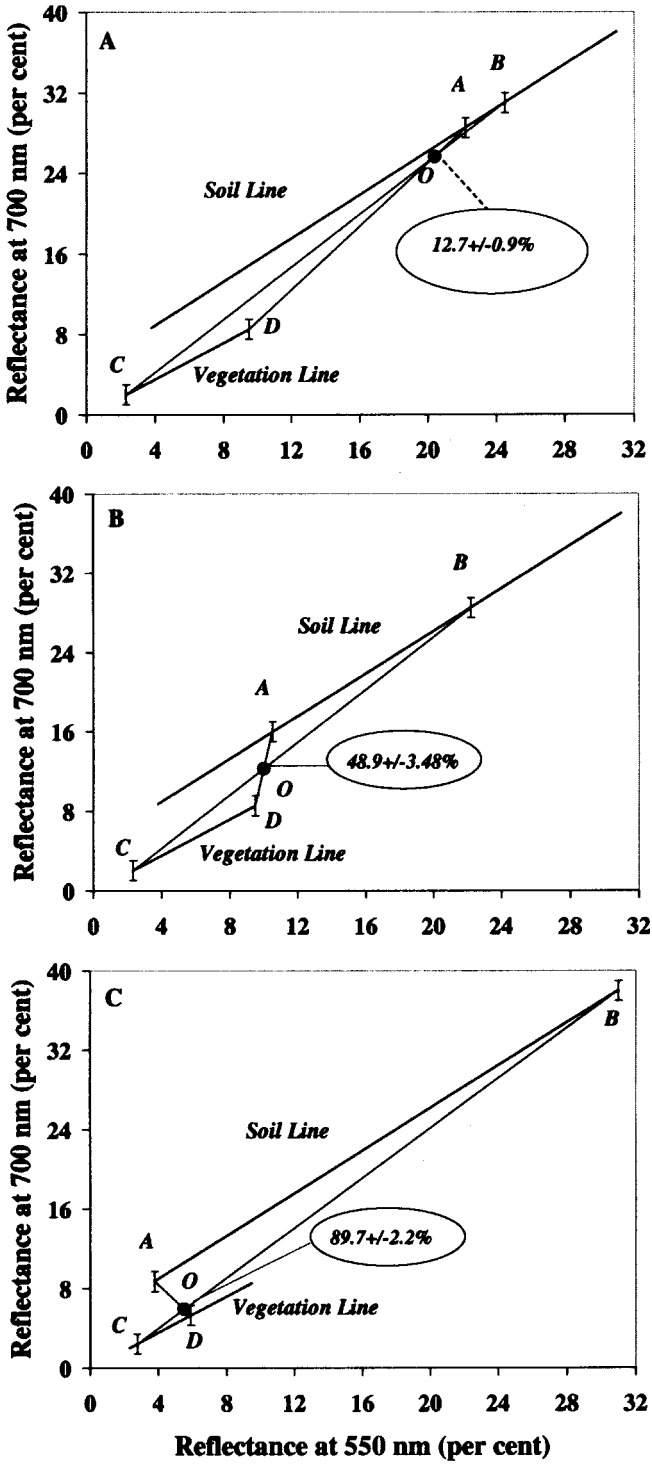

Figure 6. The positions of three actually measured wheat pixels with different vegetation fraction: (*a*) small *VF*, (*b*) moderate *VF*, and (*c*) high *VF* in R_{700} versus R_{550} spectral space.

3.3. *Vegetation fraction estimation*

To estimate *VF*:

1. vegetation and soil lines should be defined (coordinates of points E, F, G, and H in figure 5), by plotting all vegetation and soil measurements in either R_{550} versus R_{700} or R_{500} versus R_{670} spectral space and then fitting a line to the distribution of points;
2. two lengths, COB and DOA, through measured point O, vegetation line and soil line should be drawn in such a way as to make the distance between points of intersects C and D maximal for given position of point O;
3. calculate *VF* as (AO/AD + BO/BC)/2.

The estimate of *VF* for wheat was calculated as (AO/AD + BO/BC)/2 (figure 5). In both spectral spaces, relationships between estimates and actually measured *VF* were logarithmic with RMSE of less than 7.8% (figure 7). In the range of *VF* from 0% to 40%, the slope of the relationship was higher than for $VF > 50\%$. This nonlinear behaviour was due to very high LAI (when *VF* was in the range 50%–70%, LAI ranged from 4 to 6) and wheat self-shadowing. With increase of *VF*, canopy density and self-shadowing increased; the soil reflectance contribution dropped and only slightly affects canopy reflectance. As a result of it, slope of the relationships R_{670} versus R_{500} and R_{700} versus R_{550} decreased (figure 4).

The functions estimated *VF*, VF_{est}, versus measured *VF*, VF_{meas}, (i.e. retrieved from the corresponding digital images) were compared for two years of observations. Best-fit functions were found in the following forms.

Year 1997/1998:

$$VF_{\text{est}} = 29.632 \ln(VF_{\text{meas}}) - 39.425$$
$$n = 27,\ r^2 = 0.98,\ \text{RMSE} = 12.6\%$$

Year 1998/1999:

$$VF_{\text{est}} = 31.012 \ln(VF_{\text{meas}}) - 44.496$$
$$n = 90,\ r^2 = 0.97,\ \text{RMSE} = 7.8\%$$

RMSE of points measured in the 1997/1998 from a best-fit function for data obtained in 1998/1999 did not exceed 11%. Thus, the functions VF_{est} versus VF_{meas} in spaces (500, 670) and (550, 700) were found to be repeatable and stable in time for four types of wheat studied.

3.4. *Technique validation*

The proposed technique for *VF* estimation was validated by analyses done with independent datasets. For wheat in year 1997/1998, the established relationships between measured and estimated reflectances in spectral spaces (500, 670) and (550, 700) were inverted to predict *VF* in year 1998/1999. These relationships were used in the following forms.

In space (550, 700):

$$VF_{\text{pred}} = 4.045 \exp(0.0322 * VF_{\text{est}})$$
$$r^2 = 0.96,\ \text{RMSE} = 7.5\% \qquad (1)$$

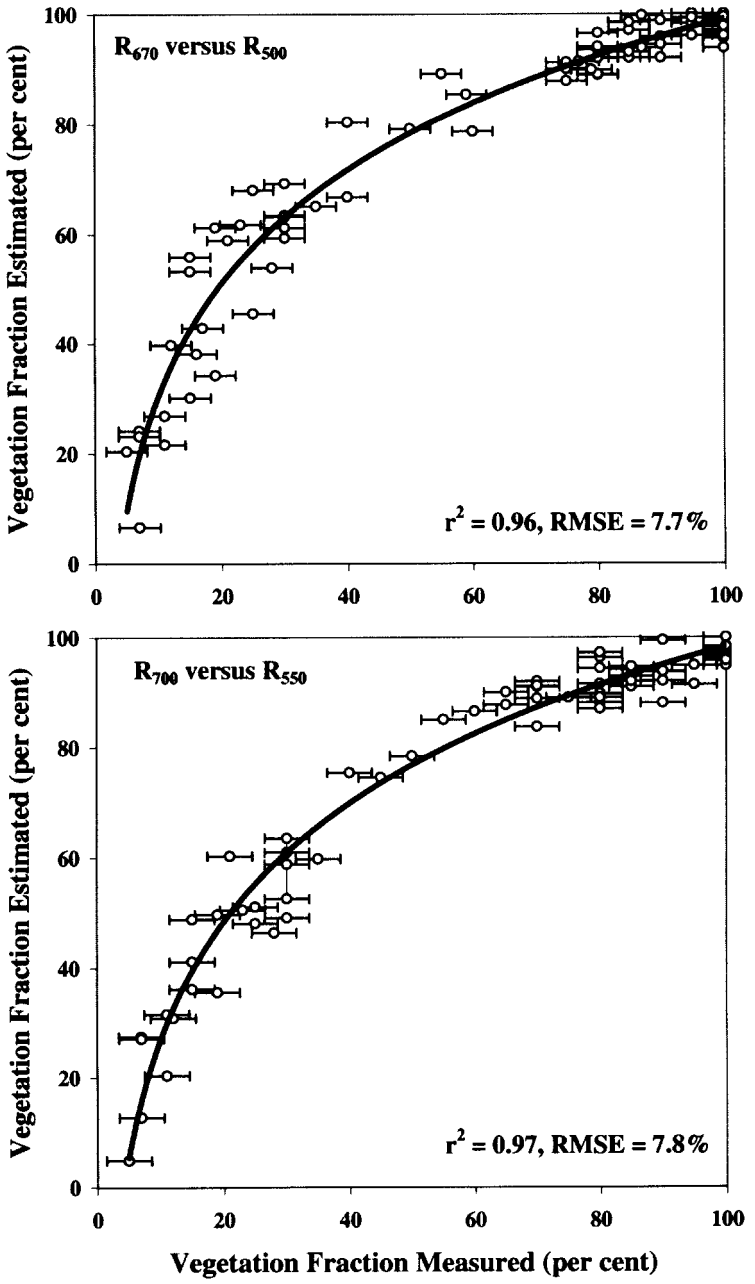

Figure 7. Wheat vegetation fraction estimated versus measured in spectral spaces (*a*) R_{670} versus R_{500} and (*b*) R_{700} versus R_{550}. Solid lines are best-fit functions.

and in space (500, 670):

$$VF_{\text{pred}} = 4.5768 \exp(0.0311 * VF_{\text{est}})$$
$$r^2 = 0.9655, \text{ RMSE} = 8.03\% \quad (2)$$

VF_{est} were calculated in spectral spaces (700, 550) and (670, 500), as described above (figure 5), for wheat in 1998/1999. These estimates then were used to calculate predicted VF using equations (1) and (2). Then, VF retrieved from digital images taken in year 1998/1999 were compared with VF predicted in spectral spaces (500, 670) and (550, 700). The determination coefficient of relationships VF_{pred} versus VF_{meas} for both spectral spaces was higher than 0.91 and error of VF prediction did not exceed 9.3% (figure 8).

The technique was also tested by independent measurements of corn reflectance carried out in Nebraska during 1998. Figure 9 shows the relationships R_{670} versus R_{500} and R_{700} versus R_{550} for corn when VF ranged between 0 and 87% and for Nebraska soils (see insets). Soil lines are the best-fit functions for soils measured at the Mead, NE research site. The soil lines represent a variety of soils measured in spring just before corn planting. We attempted to measure reflectance in as wide as possible range of soil moisture variation. Thus, we believe that the graphed soil lines show a maximal range of soil reflectance variation. Soil reflectances R_{670} and R_{500}, as well as R_{550} versus R_{700} correlated very closely (insert, figure 9).

For the corn canopy, the range of reflectance variation was narrower than for wheat, but nevertheless, VF variation was very distinctive in both spectral spaces. Red and blue reflectances for almost closed corn canopies were very small (2.1% to 2.7%, respectively), as was the case for wheat. Measured reflectances were not scattered widely, depicting a narrow range of soil brightness during the 1998 growing season. In both spaces, reflectances R_{670} and R_{500}, as well as R_{550} versus R_{700} correlated very closely; relationships between them in both spaces were fairly linear ($r^2 = 0.96$, RMSE $< 0.25\%$).

Maximal VF for corn studied was 87%; thus, we could not establish a true vegetation line for corn. Therefore, in both spectral spaces, we employed the vegetation lines that were formed by the reflectance from wheat with $VF = 100\%$ (figures 2(*a*) and (*b*)). The maximal difference between reflectance of corn with $VF = 87\%$ and the vegetation line for wheat ($VF = 100\%$) was 0.6% at 670 nm and 1% at 700 nm.

The results of the comparison between estimated and actually measured VF are shown in figure 10. Relationships between estimated and measured VF were found to be linear in both spaces with $r^2 = 0.82$ in (550, 700) space and $r^2 = 0.92$ in (500, 670) space. RMSE of VF prediction did not exceed 6.6% for (500, 670) space and 9.7% for (550, 700) space.

4. Discussion

Spectral features of closed canopy reflectance strongly resemble those of leaves. At leaf level in a wide range of chlorophyll content, strong covariance exists between R_{500} and R_{670} (Gitelson and Merzlyak 1996, Gitelson *et al.* 1996, Lichtenthaler *et al.* 1996) and between R_{550} and R_{700} (Chappelle *et al.* 1992, Gitelson and Merzlyak 1994a, McMurtrey III *et al.* 1994, Gitelson *et al.* 1996, Lichtenthaler *et al.* 1996). In spectral spaces (500, 670) and (550, 700), reflectance of closed canopy form distinctive vegetation lines with a slope lower than that of soil line. For a closed canopy, the information content of crop reflectance spectra became very low; reflectance in the blue and the red ranges provide almost the same information. Virtually the same information content exists in the green range and in the red edge range near 700 nm. For a closed canopy in the visible spectrum, in reality, two independent spectral bands exist: (1) either near 500 nm or around 670 nm; and (2) either around 550 nm or near 700 nm. The same information content in leaf-reflectance spectra in the

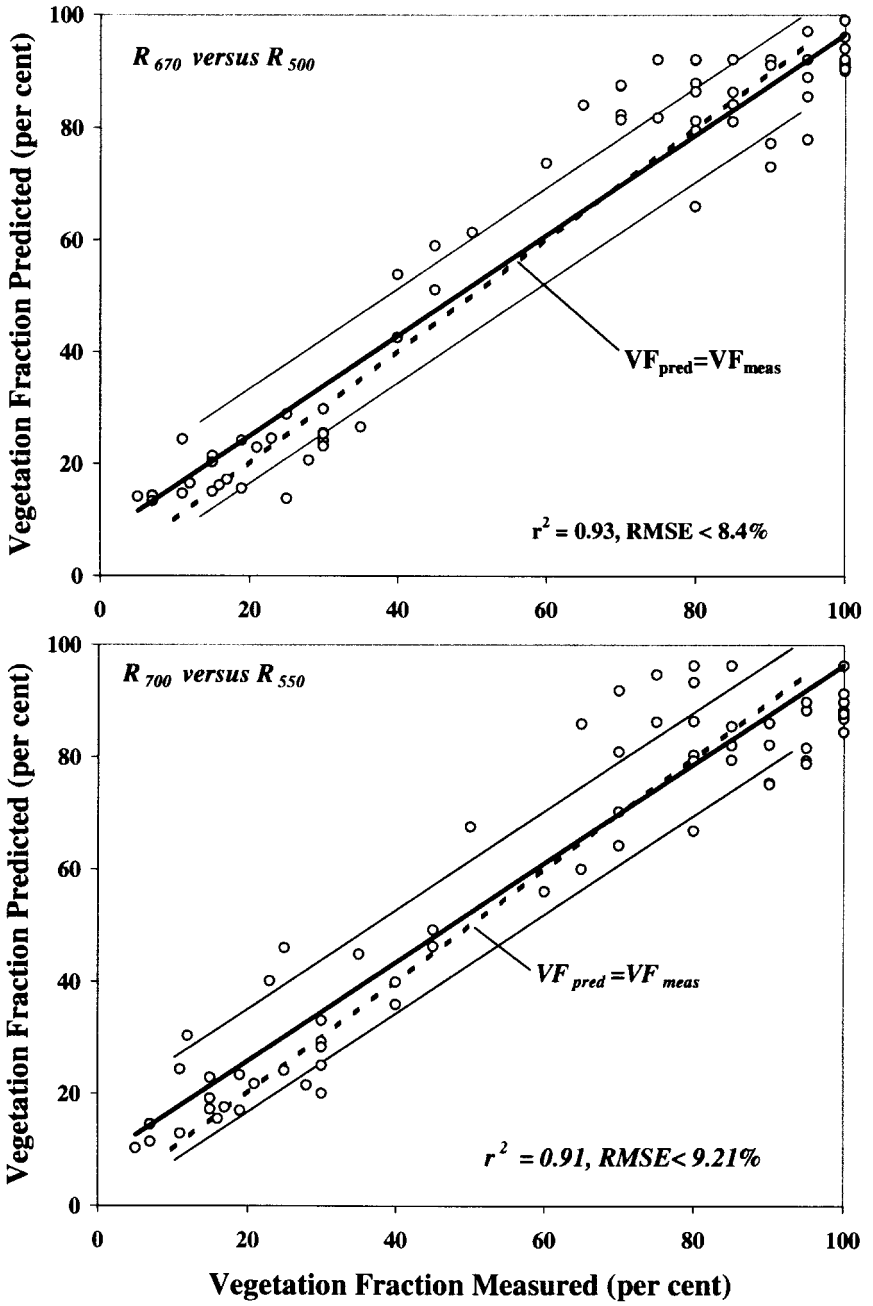

Figure 8. Wheat vegetation fraction predicted from spectral data taken in 1998/1999 versus measured values. Predicted VF was calculated using equations (1) and (2) established for the 1997/1998 dataset. Solid lines are best-fit functions; in space R_{700} versus R_{550}: $VF_{\text{pred}} = 0.89VF_{\text{meas}} + 7.1$; in space R_{670} versus R_{500}: $VF_{\text{pred}} = 0.88VF_{\text{meas}} + 8.2$. Thin lines show root-mean square errors of sample points from the linear relationship VF_{pred} versus VF_{meas}. Dotted lines are $VF_{\text{pred}} = VF_{\text{meas}}$.

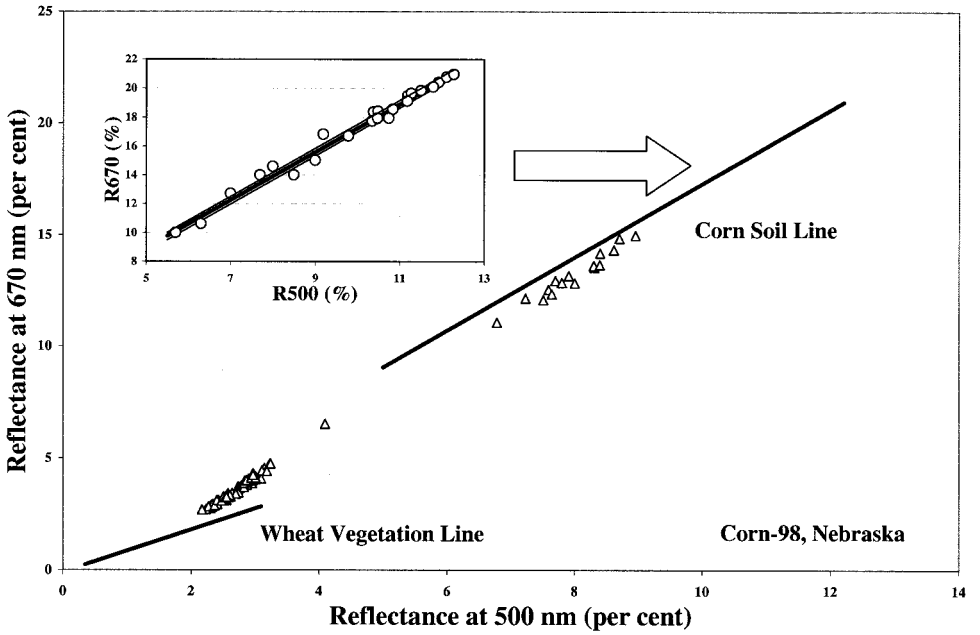

(*a*)

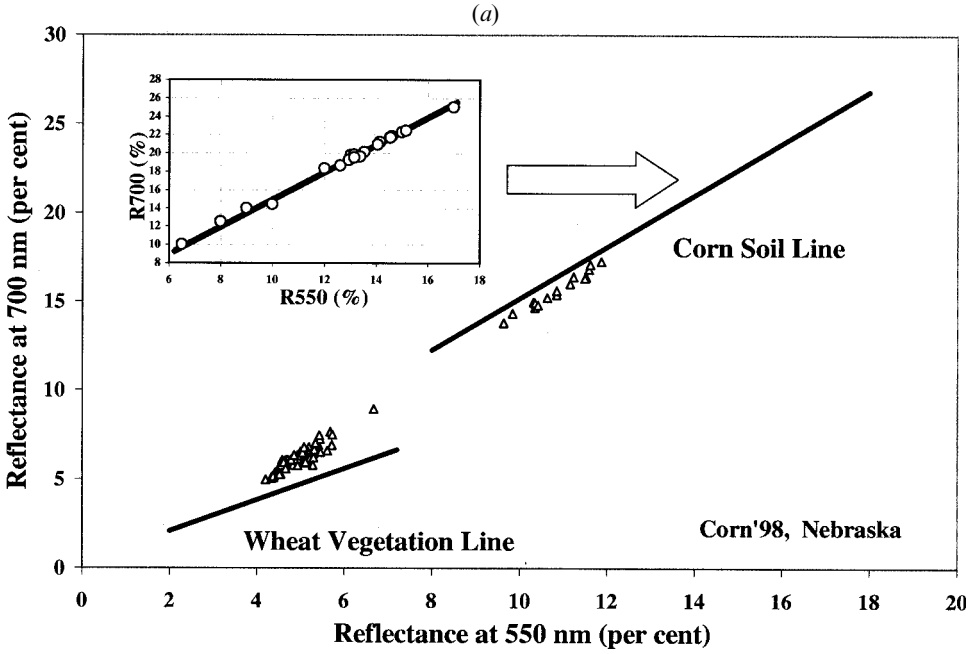

(*b*)

Figure 9. Reflectance (*a*) R_{670} versus R_{500} and (*b*) R_{700} versus R_{550} of cornfields measured in Nebraska in 1998. Vegetation fraction ranged from 0 to 87%. Vegetation lines established for wheat with $VF = 100\%$ (figure 2) were used. Soils of very different types and wetness (inserts) form soil lines in both spectral spaces.

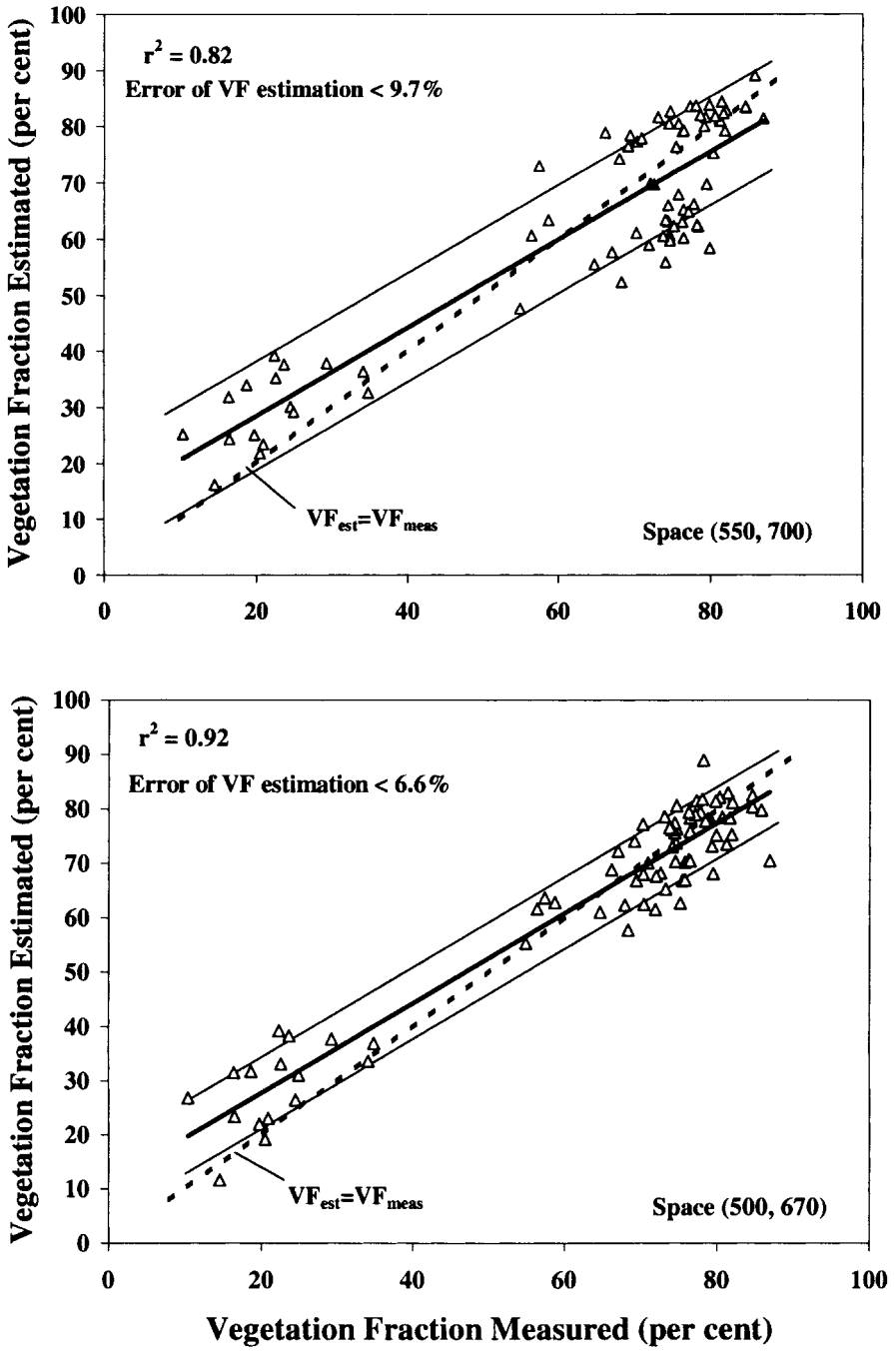

Figure 10. Comparison between vegetation fractions predicted and retrieved from digital images for cornfields measured in Nebraska in 1998. Root-mean square error of VF prediction did not exceed 9.2%. Solid lines are best-fit functions; in space R_{700} versus R_{550}: $VF_{\text{pred}} = 0.83\,VF_{\text{meas}} + 11.2$, in space R_{670} versus R_{500}: $VF_{\text{pred}} = 0.79\,VF_{\text{meas}} + 12.8$. Thin lines show root-mean square errors of sample points from the linear relationship VF_{pred} versus VF_{meas}. Dotted lines are $VF_{\text{pred}} = VF_{\text{meas}}$.

visible range was found earlier (Gitelson *et al.* 1996). Therefore, the vegetation line concept, presented in this work, is grounded in the fundamental spectral characteristics of leaves.

It is assumed that the position of a given sample (as defined by R_{500} and R_{670} as well as R_{550} and R_{700}) within the soil and vegetation line-based two-dimensional spectral construct is a measure of *VF*. As such, we suggest using an average of ratios calculated as the distance of the measured point from the soil line to the distance between the soil and vegetation lines for maximal and minimal possible soil brightness. The procedure accounts for at least to some extent, the possible range of soil and vegetation brightness variation for each measured canopy.The proposed spectral spaces are very different from the more typical NIR-Red (Richardson and Weigand 1977) and Green-Red approaches (Pickup *et al.* 1993). In spectral spaces (500, 670) and (550, 700), the perpendicular distance from the soil line is an illogical measure of *VF*. As can be seen from figures 4 and 9, with an increase in *VF*, both reflectances decreased and shifted toward the portion of the vegetation line that is not only opposite the soil line but also is located quite close to the origin. The proposed technique allows accurate assessment of *VF* for two types of crops with very different density in a wide range of soil brightness. Nevertheless, many questions should be addressed in further studies.

Attention should be given to those factors that contribute to both the length of the vegetation line and its slope. The vegetation line length depends upon vegetation greenness (pigment content and composition), canopy density and structure. The wider the variation of these factors, the longer the vegetation line. The contribution of canopy density to length of wheat vegetation line was estimated. With increase of LAI from 7–8 to 12, reflectance of closed canopy in the blue and the red ranges decreased from 2.3% to 0.8%. Reflectance in the green and the red edge ranges was more sensitive to canopy density, decreasing from 6.8% to 3.2% with increase in LAI. Thus, it can be concluded that in space (500, 670) at least 60% of closed canopy reflectance variation may be attributed to variation in LAI, and in space (550, 700) this contribution exceeded 70%.

The remaining variation in closed canopy reflectance is due to change in wheat greenness and canopy structure. Chlorophyll content in leaves, as measured by means of an LI-1800IS integrating sphere, in closed canopy ranged from 30 to 45 $mg\,m^{-2}$. The red and the blue reflectances of the wheat leaves were virtually unchanged. Thus, we cannot expect a significant contribution of chlorophyll variation to vegetation line length in (500, 670) spectral space. Variation of reflectance in the green and the red edge ranges was higher, but not exceeded 1.5%. Thus, in space (550, 700), more than 95% of vegetation line length may be attributed to variation in LAI and chlorophyll content. The much higher length of vegetation line in (550, 700) than in (500, 670) space is due to higher sensitivity of reflectance in these spectral bands to LAI and chlorophyll content.

Change in canopy structure may also affect reflectance of the canopy. In space (500, 670), beside variation in LAI, probably, it is the main contributor to length of vegetation line. Even small variation in specular reflectance would be a significant contribution to vegetation line length in (500, 670) space where total variation of reflectance did not exceed 2.5%.

For a closed green canopy, absorption by pigments is the main factor governing synchronous decrease of reflectances R_{500} and R_{670} as well as R_{550} and R_{700}, and the slope of vegetation lines in both spectral spaces was close to one. The same slope

of these relationships was found in leaves of several non-related species from different climatic zones (Chappelle *et al.* 1992, Gitelson and Merzlyak 1994a,b, 1996, 1997, McMurtrey III *et al.* 1994, Lichtenthaler *et al.* 1996, Schepers *et al.* 1996). In spaces (500, 670) and (550, 700) points representing pepper plants with 100% *VF* were situated just on the wheat vegetation line (Rundquist *et al.* 2000). Recently obtained reflectance data (not shown) for closed corn, soybean and sorghum canopies also show that points fit well with the wheat vegetation line in both spaces. So, it is not likely that the slope of the vegetation line will vary significantly for different plant species and the vegetation line will still represent reflectance of vegetation with different density and chlorophyll content.

Soils of very different types (e.g. dark in Nebraska and light in Israel) form a soil line in both (500, 670) and (550, 700) spectral spaces. The slopes of the soil lines remained almost the same (figure 11). In space (500, 670), reflectance of soils in Nebraska at 670 nm was about 3% lower than that of soil in Israel; as a result, the soil line for corn was shifted almost in parallel toward higher R_{500} values. Surprisingly, in space (550, 700) soil lines measured in Nebraska and in Israel practically coincided.

Any technique using the index approach is based on the assumption that consistent relationships exist between the *VF* and vegetation index value for different plant species and over time. We tried to test this assumption for corn and wheat with extremely different densities: LAI reached 12 in irrigated wheat and did not exceed 2.7 in corn. The position of a sample in both spectral spaces depended not only on *VF*, vegetation greenness and soil brightness, but also on LAI. For $VF > 75\%$, a large difference in crop density manifested itself as a difference in reflectance at 670 nm (figure 12). For the same *VF*, reflectance of wheat at 670 nm was lower than that of corn and distance between a point and the vegetation line was smaller. Thus, apparent *VF* of wheat was higher than in corn. It may be explained by a strong self-shadowing effect that was significant in wheat and caused nonlinear behaviour of estimates versus actually measured *VF* (figure 7). In the corn and the sorghum (with LAI up to 3.6) and in wheat (with LAI up to 5) relationships R_{550} versus R_{700} and R_{500} versus R_{670} were fairly linear. Comparison of results of corn *VF* retrieval for two years observation showed that the difference in density (LAI = 2.7 in 1998 and 3.6 in 1999 and 2000) did not affect *VF* estimation by means of suggested technique (Rundquist *et al.* in preparation).

Further research is under way to investigate how slope and length of a vegetation line depends on vegetation type. Much attention is given to the relationship between magnitude of reflectance R_{500}, R_{550}, R_{670}, and R_{700} and canopy density for different species.

5. Conclusions

1. Reflectance of the wheat with 100% vegetation fraction, despite various canopy structures and pigment contents, forms a vegetation line defined by close linear relationships of reflectances R_{700} versus R_{550}, and R_{670} versus R_{500}. The position and orientation of the lines in two-dimensional spectral space were repeatable for four types of wheat during two years of observations. Soils of very different types and wetness form soil lines in the (500, 670) and (550, 700) spectral spaces. The soil lines have also proven to be repeatable over the course of two years of data collection.

2. Two-dimensional spectral space, as defined and constrained by soil and vegetation lines, includes all possible canopy reflectances with *VF* ranging from 0 to

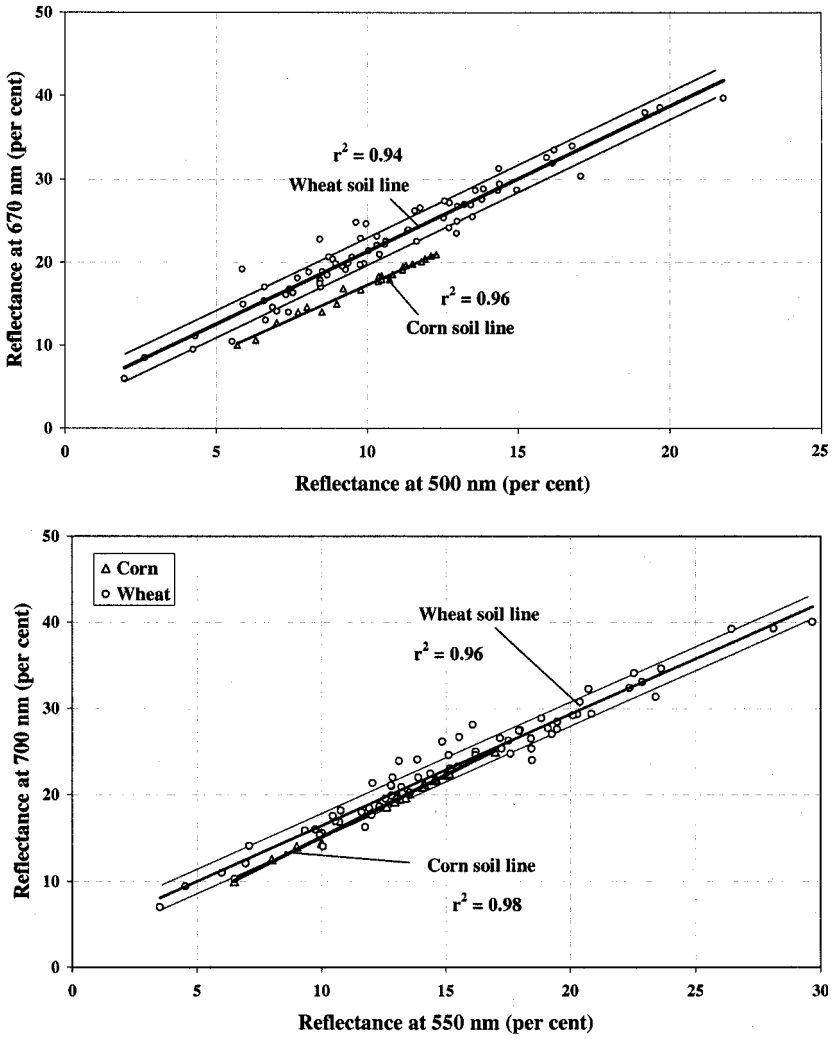

Figure 11. Soil reflectance measured in Israel (wheat soil line) and in Nebraska (corn soil line) in spectral spaces R_{670} versus R_{500} and R_{700} versus R_{550}. Solid lines are best-fit functions. In space R_{670} versus R_{500} wheat soil line: $R_{670} = 1.75R_{500} + 3.8$, corn soil line: $R_{670} = 1.65R_{500} + 0.75$. In space R_{700} versus R_{550} wheat soil line: $R_{700} = 1.29R_{550} + 3.5$, corn soil line: $R_{700} = 1.49R_{550} + 0.04$. Thin lines show root-mean square errors of sample points from the linear relationship R_i versus R_j.

100%. We suggest using the location of reflectance in these spectral spaces as a quantitative measure of *VF*. The relationship between estimated and measured *VF* was found to be repeatable and stable for four wheat types (two years of observations) and space (sampling has been done in variety of sample sites and fields). Predicted *VF* was proportional to measured *VF* with RMSE of less than 10%. For the independent data set in corn, excellent correspondence was found between predicted and measured vegetation fraction values for a variety of soil types.

3. The spectral features of wheat and corn reflectance revealed in this study would conceivably be comparable with other vegetation types. It should be stressed

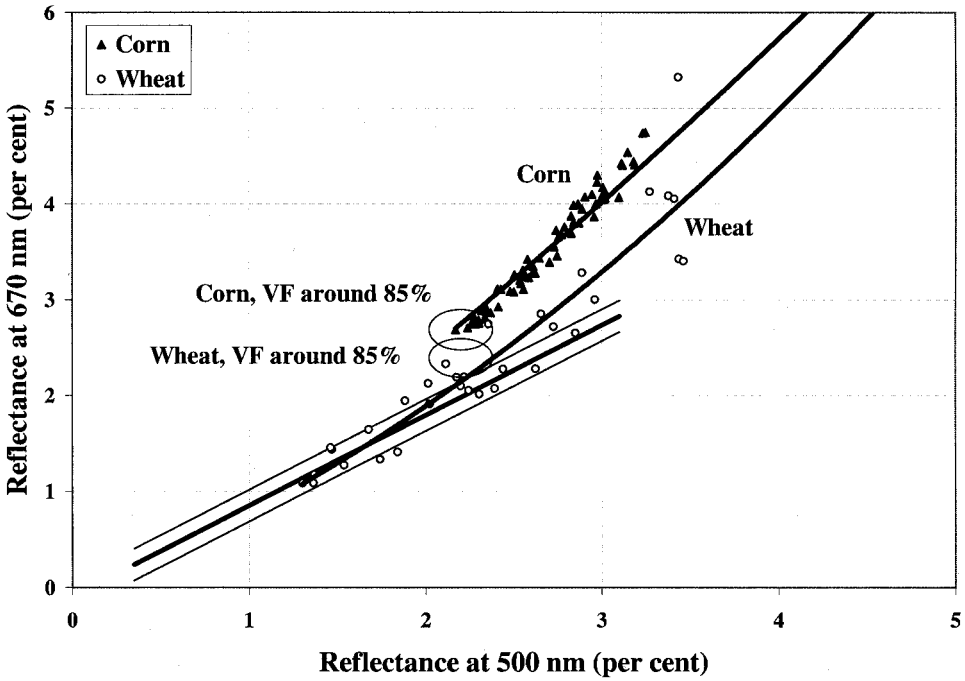

Figure 12. Reflectance of wheat and corn with vegetation fraction exceeding 60%. For the same vegetation fraction around 85%, reflectance of wheat at 670 nm was lower than that of corn, and distance between the point and the vegetation line was smaller. Thus, apparent *VF* of wheat was higher than in corn.

however, that the applicability of the proposed techniques to other vegetation types must yet be verified. In order to broaden the models offered in this work and to devise comprehensive algorithms for monitoring vegetation fraction by use of remote sensing, more studies of closed canopy reflectance are required.

Acknowledgments

The authors are very grateful for assistance provided by Galina Keydan and Rick Perk, UNL and Yoav Zur, Ben-Gurion University of the Negev, Israel. We also thank an anonymous reviewer for valuable and constructive suggestions and criticism.

References

ADAMS, J. B., and SMITH, M. O., 1986, Spectral mixture modelling: A new analysis of rock and soil types at the Viking Lander 1 site. *Journal Geophysical Research*, **91**, 8098–8112.

ASRAR, G., FUCHS, M., KANEMASU, E. T., and HATFIELD, J. L., 1984, Estimating absorbed photosynthetic radiation and leaf area index from spectral reflectance in wheat. *Agronomy Journal*, **76**, 300–306.

BARET, F., GUYOT, G., and MAJOR, D., 1989, TSAVI: A vegetation index which minimizes soil brightness effects on LAI and APAR estimation. *12th Canadian Symposium on Remote Sensing and IGARSS'90, Vancouver, Canada, 10–14 July 1989.*

BARET, F., JACQUEMOUD, S., and HANOCQ, J. F., 1993, The soil line concept in remote sensing. *Remote Sensing Reviews*, **7**, 65–82.

BARET, F., CLEVERS, J. G. P. W., and STEVEN, M. D., 1995, The robustness of canopy gap

fraction estimates from red and near-infrared reflectances: A comparison of approaches. *Remote Sensing of Environment*, **54**, 141–151.

CHAPPELLE, E. W., KIM, M. S., and MCMURTREY III, J. E., 1992, Ratio analysis of reflectance spectra (RARS): An algorithm for the remote estimation of the concentrations of chlorophyll a, chlorophyll b, and carotenoids in soybean leaves. *Remote Sensing of Environment*, **39**, 239–247.

COLWELL, J. E., 1974, Vegetation canopy reflectance. *Remote Sensing of Environment*, **3**, 175–183.

DAUGHTRY, C. S. T., BAUER, M. E., CRECELIUS, D. W., and HIXSON, M. M., 1980, Effects of management practices on reflectance of spring wheat canopies. *Agronomy Journal*, **72**, 1055–1060.

DERRY, D., 2000, Monitoring corn development via close-range and aerial remote sensing. Masters Thesis, Department of Geography, University of Nebraska-Lincoln.

GARCIA-HARO, F. J., GILABERT, M. A., and MELIA, J., 1996, Linear spectral mixture modelling to estimate vegetation amount from optical spectral data. *International Journal of Remote Sensing*, **17**, 3373–3400.

GITELSON, A., and MERZLYAK, M. N., 1994a, Spectral reflectance changes associated with autumn senescence of *Aesculus hippocastanum* L. and *Acer platanoides* L. leaves. Spectral features and relation to chlorophyll estimation. *Journal of Plant Physiology*, **143**, 286–292.

GITELSON, A., and MERZLYAK, M. N., 1994b, Quantitative estimation of chlorophyll using reflectance spectra: Experiments with autumn chestnut and maple leaves. *Journal of Photochemistry and Photobiology (B)*, **22**, 247–252.

GITELSON, A., and MERZLYAK, M. N., 1996. Signature analysis of leaf reflectance spectra: Algorithm development for remote sensing of chlorophyll. *Journal of Plant Physiology*, **148**, 494–500.

GITELSON, A., and MERZLYAK, M. N., 1997, Remote estimation of chlorophyll content in higher plant leaves. *International Journal of Remote Sensing*, **18**, 291–298.

GITELSON, A., KAUFMAN, Y. J., and MERZLYAK, M. N., 1996, Use of a green channel in remote sensing of global vegetation from EOS-MODIS. *Remote Sensing of Environment*, **58**, 289–298.

GITELSON, A., GRITS, U., STARK, R., RUNDQUIST, D., and KAUFMAN, Y. J., 2000. Novel algorithms for remote estimation of vegetation fraction. *Conference Proceedings of the Second International on Geospatial Information in Agriculture and Forestry Conference, Lake Buena Vista, Florida, 10–12 January, 2000*, **2**, pp. 1–8.

GITELSON, A., KAUFMAN, Y. J., STARK, R., and RUNDQUIST, D., 2002, Novel algorithms for remote estimation of vegetation fraction. *Remote Sensing of Environment*, **80**, 76–87.

HOLBEN, B. N., 1986, Characteristics of maximum value composite images for temporal AVHRR data. *International Journal of Remote Sensing*, **7**, 1417–1437.

HUETE, A. R., 1988, A soil-adjusted vegetation index (SAVI). *Remote Sensing of Environment*, **25**, 295–309.

HUETE, A. R., JUSTICE, C., and LIU, H., 1994, Development of vegetation and soil indices for MODIS-EOS. *Remote Sensing of Environment*, **49**, 224–234.

JACKSON, R. D., and EZRA, C. E., 1985, Spectral response of cotton to suddenly induced water stress. *International Journal of Remote Sensing*, **6**, 177–185.

JACKSON, R. D., CLARKE, T. R., and MORAN, M. S., 1992, Bidirectional calibration results for 11 Spectralon and 16 $BaSO_4$ reference reflectance panels. *Remote Sensing of Environment*, **40**, 231–239.

KANEMASU, E. T., 1974, Seasonal canopy reflectance patterns of wheat, sorghum, and soybean. *Remote Sensing of Environment*, **3**, 43–47.

KAUFMAN, Y. J., 1989, The atmospheric effect on remote sensing and its corrections. In *Theory and Application of Optical Remote Sensing*, edited by G. Asrar (New York: John Wiley & Sons, Inc.), pp. 336–428.

KAUFMAN, Y. J., and TANRE, D., 1992, Atmospherically Resistant Vegetation Index (ARVI) for EOS-MODIS. *IEEE Transactions on Geoscience and Remote Sensing*, **30**, 261–270.

KIM, M. S., DAUGHTRY, C. S. T., CHAPPELLE, E. W., MCMURTREY, J. E., and WALTHALL, C. L., 1994, The use of high spectral resolution bands for estimating absorbed photosynthetically active radiation. *Proceedings 6th International. Symposium Physical Measurements and Signatures in Remote Sensing, Val d'Isere, France, 1994*, pp. 299–306.

LELONG, C. C. D., PINET, P. C., and POILVE, H., 1998, Hyperspectral imaging and stress mapping in agriculture: A case study on wheat in Beauce (France). *Remote Sensing of Environment*, **66**, 179–191.

LICHTENTHALER, H. K., 1987, Chlorophyll and carotenoids: Pigments of photosynthetic biomembranes. *Methods in Enzymology*, **148**, 331–382.

LICHTENTHALER, H., GITELSON, A., and LANG, M., 1996, Non-destructive determination of chlorophyll content of leaves of a green and an aurea mutant of tobacco by reflectance measurements. *Journal of Plant Physiology*, **148**, 483–493.

MCMURTREY III, J. E., CHAPPELLE, E. W., KIM, M. S., MEISINGER, J. J., and CORP, L. A., 1994, Distinguishing nitrogen fertilization levels in field corn (Zea mays L.) with actively induced fluorescence and passive reflectance measurements. *Remote Sensing of Environment*, **47**, 36–44.

MERZLYAK, M. N., GITELSON, A., CHIVKUNOVA, O. B., and RAKITIN, Y. *R*., 1999, Non-destructive optical detection of pigment changes during leaf senescence and fruit ripening. *Physiologia Plantarum*, **106**, 135–141.

MORAN, M. S., INOUE, Y., and BARNES, E. M., 1997, Opportunities and limitations for image-based remote sensing in precision crop management. *Remote Sensing of Environment*, **61**, 319–346.

MYNENI, R. B., HALL, F. G., SELLERS, P. S., and MARSHAK, A. L., 1995, The interpretation of spectral vegetation indexes. *IEEE Transactions on Geoscience and Remote Sensing*, **33**, 481–486.

MYNENI, R. B., NEMANI, R. R., and RUNNING, S. W., 1997, Estimation of global leaf area index and absorbed par using radiative transfer models. *IEEE Transactions on Geoscience and Remote Sensing*, **35**, 1380–1393.

PICKUP, G., CHEWINGS, V. H., and NELSON, D. J., 1993, Estimating changes in vegetation cover over time in arid rangelands using Landsat MSS data. *Remote Sensing of Environment*, **43**, 243–263.

PRICE, J. C., 1994, How unique are spectral signatures? *Remote Sensing of Environment*, **49**, 181–186.

RICHARDSON, A. J., and WIEGAND, C. L., 1977, Distinguishing vegetation from soil background information. *Photogrammetric Engineering and Remote Sensing*, **43**, 1541–1552.

ROBERTS, D. A., SMITH, M. O., and ADAMS, J. B., 1993, Green vegetation, nonphotosynthetic vegetation, and soils in AVIRIS data. *Remote Sensing of Environment*, **44**, 255–269.

ROBERTS, D. A., GREEN, R. O., and ADAMS, J. B., 1997, Temporal and spatial patterns in vegetation and atmospheric properties from AVIRIS. *Remote Sensing of Environment*, **62**, 223–240.

RUNDQUIST, D., RAMIREZ, J., and GITELSON, A., 2000, The effect of extreme background conditions on reflectance of vegetation and estimation of vegetation fraction. In *Proceedings of the Second International on Geospatial Information in Agriculture and Forestry Conference, Lake Buena Vista, Florida, 10–12 January, 2000*, Vol. **2**, 59–65.

SANDMEIER, S., MULLER, C., HOSGOOD. B., and ANDREOLI, G., 1998, Physical mechanisms in hyperspectral BRDF data of grass and watercress. *Remote Sensing of Environment*, **66**, 222–233.

SELLERS, P. J., 1985, Canopy reflectance, photosynthesis and transpiration. *International Journal of Remote Sensing*, **6**, 1335–1372.

SCHEPERS, J. S., BLACKMER, T. M., WILHELM, W. W., and RESENDE, M., 1996, Transmittance and reflectance measurements of corn leaves from plants with different nitrogen and water supply. *Journal of Plant Physiology*, **148**, 523–529.

STARK, R., and GITELSON, A., 1999, Light distribution in field communities of irrigated wheat plants. In *Proceedings of the Fourth International Airborne Remote Sensing Conference and Exhibition/21st Canadian Symposium on Remote Sensing, Ottawa, Ontario, Canada, 21–24 June 1999*, pp. 321–326.

STARK, R., and GITELSON, A., 2000, Radiation regime in irrigated wheat. *Proceedings of the Second International on Geospatial Information in Agriculture and Forestry Conference, Lake Buena Vista, Florida, 10–12 January 2000*, **2**, pp. 89–96.

STEVEN, M. D., BISCOE, P. V., JAGGARD, K. W., and PARUNTU, J., 1986, Foliage cover and radiation interception. *Field Crops Research*, **13**,75–87.

TUCKER, J. C., 1979, Red and photographic infrared linear combination for monitoring vegetation. *Remote Sensing of Environment*, **8**, 127–150.

TUCKER, C. J., HOLBEN, B. N., ELGIN, J. H. JR., and MCMURTREY III, J. E., 1981, Remote sensing of total dry-matter accumulation in winter wheat. *Remote Sensing of Environment*, **11**, 171–189.

USTIN, S. L., HART, Q. J., DUAN, L., and SCHEER, G., 1996, Vegetation mapping on hardwood rangelands in California. *International Journal of Remote Sensing*, **17**, 3015–3036.

VERSTRAETE, M. M., PINTY, B., and MYNENI, R. B., 1996, Potential and limitations of information extraction on the terrestrial biosphere from satellite remote sensing. *Remote Sensing of Environment*, **58**, 201–214.

YODER, B. J., and WARING, R. H., 1994, The normalized difference vegetation index of small Douglas-fir canopies with varying chlorophyll concentrations. *Remote Sensing of Environment*, **49**, 81–91.